Malaysian Journal of Analytical Sciences
(MJAS)
Published by Malaysian Analytical Sciences Society
ANALIS
Persatuan Sains Analisis Malaysia

SYNTHESIS, ELECTROCHEMICAL ANALYSIS AND DFT CALCULATION OF NEW ALKOXYLATED-CHALCONE AS SEMICONDUCTOR MATERIAL

(Sintesis, Analisis Elektrokimia dan Pengiraan DFT bagi Alkoksi-Kalkon Sebagai Bahan Semikonduktor)

Syaharil Saidin[1], Wan M. Khairul[1*], Rafizah Rahamathullah[2]

[1]*Faculty of Science and Marine Environment,*
Universiti Malaysia Terengganu, 21030, Kuala Nerus, Terengganu, Malaysia
[2]*Faculty of Engineering Technology,*
Universiti Malaysia Perlis,
Level 1, Block S2, UniCITI Alam Kampus, Sungai Chuchuh, Padang Besar, 02100 Perlis, Malaysia

[*]*Corresponding author: wmkhairul@umt.edu.my*

Received: 13 March 2022; Accepted: 18 May 2022; Published: 30 October 2022

Abstract

A new alkoxylated-chalcone derivative displaying donor(D)-π-acceptor(A) system was successfully synthesized via Claisen-Schmidt condensation to be integrated as organic semiconductor material. The correlation between electronic, optical properties, electrochemical and DFT calculation of the designated system were assessed in thorough. This alkoxylated-chalcone (**OCT-CHAL**) reveals an absorption band at λ_{max} 312 nm with molar coefficient of *ca.* 10^5 L mol^{-1} cm^{-1} which corresponding to π-π^* transition. The optical band gap gives the value of 3.40 eV which shows good agreement with the value of energy level between HOMO and LUMO for theoretical calculation. Meanwhile, this derivative also reveals good thermal stability up to 200 ℃ with total mass loss at 97 %. In turn, the electrochemical behaviour of **OCT-CHAL** was investigated and exhibited redox potential with the values of 2.40 V for oxidation potential while the reduction potential exhibited at value of -1.72 V as quasi-reversible reduction. From the outcome, the existence of conjugation effect on chalcone moiety with ideal relation between the experimental and theoretical approach provides good support of being a potential candidate in organic semiconductor material for advance material application.

Keywords: alkoxy, chalcone, bandgap, DFT, electrochemistry

Abstrak

Terbitan alkoksi-kalkon baharu yang memaparkan sistem penderma(D)-π-penerima(D) telah berjaya disintesis melalui kaedah kondensasi Claisen-Schmidt untuk diintegrasikan sebagai bahan organik semikonduktor. Perkaitan antara elektronik, sifat optik, elektrokimia dan pengiraan DFT bagi sistem yang direkabentuk telah dinilai secara menyeluruh. Alkoksi-kalkon (**OCT-CHAL**) ini menunjukkan jalur serapan pada λ_{mak} 312 nm dengan pekali molar 10^5 L mol^{-1} cm^{-1} yang selari dengan peralihan π-π^*. Nilai jurang jalur optik memberikan nilai 3.40 eV yang mana keputusannya menunjukkan nilai yang selari dengan nilai aras tenaga antara HOMO dan LUMO bagi pengiraan teori. Sementara itu, terbitan ini juga menunjukkan kestabilan terma yang baik sehingga 200 ˚C dengan jumlah jisim yang hilang sebanyak 97 %. Selanjutnya sifat elektrokimia bagi **OCT-CHAL** telah dikaji dan menunjukkan keupayaan redoks dengan nilai 2.40 V untuk potensi pengoksidaan manakala potensi penurunan adalah pada nilai -1.72 V sebagai penurunan kuasi-terbalik. Daripada keputusan yang diperolehi, kehadiran kesan konjugasi pada moiti kalkon dengan hubungan yang baik antara kaedah eksperimen dan teori memberikan sokongan yang baik untuk menjadi calon berpotensi dalam bahan organik semikonduktor bagi aplikasi bahan termaju.

Kata kunci: alkoksi, kalkon, jurang jalur, DFT, Elektrokimia

Introduction

In recent years, the development of organic semiconductor has been extensively explored due to its electronic delocalization in π-orbital system in optimizing the efficiencies of various application in electrical and optoelectronic application [1]. The materials have been extensively studied as a small molecule and polymer and mostly comprised of carbon and hydrogen atom in their molecular structure where the mobility of electron transfer is occurred within the molecule. Considering to the ability in transferring electron, chalcone backbone has been introduced as an organic material which fulfilled this criterion [2,3]. Chalcone, known as 1,3-diphenyl-2-propen-1-one is a molecule that consists of two phenyl rings with α, β-unsaturated ketone (C=C-C=O) moiety in their molecular build-up has attracted considerable attention among researchers due to its electronic properties according to the presence of π-conjugated system in their molecular backbone [4]. Generally, a conjugated system would generate a cloud of delocalized electron merging by π-electron system which enables the flowing of electron along the molecular framework thus activates its potential as charge carrier mobility [5]. Meanwhile, chalcone is considered as a molecule with high charge transfer mobility as it exhibits intramolecular charge transfer (ICT) properties and is known as considerably highly emissive molecule as reported previously [6]. However, the elections of substituents towards the terminals of the phenyl rings would determine their contribution as good charge transfer ability [7], and appropriate selection of these substituents lead to the development of application such as in optoelectronics particularly in potential non-linear optical interests [8].

In this context, the chalcone based compound is introduced with the attachment of ideal substituents to develop a molecule with donor-π-acceptor (D-π-A) system in enhancing the ICT properties of the molecule [9]. The introduction of alkoxy chain towards chalcone based molecule was believed in lowering the energy band gap due to the steric bulkiness of the compound [10], thus enables it to lie in typical band gap range of semiconducting materials. Various physicochemical evaluations were accomplished via cyclic voltammetry (CV) technique in order to study their electrochemical properties and behaviour to establish their potentiality as semiconducting materials. As part of our studies in this area, a model molecule of new alkoxylated-based chalcone derivative namely, 1-(4-octoxyphenyl)-3-[4-(trifluoromethyl)phenyl]prop-2-en-1-one **(OCT-CHAL)** featuring D-π-A system presented in Figure 1 was successfully designed, synthesized and demonstrated as a semiconducting material as reported herein.

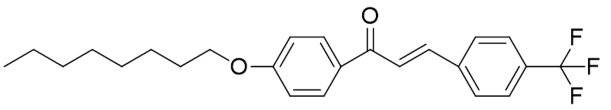

OCT-CHAL

Figure 1. Molecular structure of **OCT-CHAL** derivative

Materials and Methods

4-hydroxyacetophenone, 1-bromooctane, potassium carbonate, 4-trifluoromethylbenzaldehyde, hexane, dimethylformamide (DMF), hexane, ethyl-acetate, sodium hydroxide (NaOH), anhydrous hydrochloric acid (HCl), sodium sulphate and silica gel blue were commercially purchased form standard commercial suppliers namely Sigma Aldrich, Merck, Fisher Scientific and R&M Chemical without any further purification procedures were performed. The reaction was carried out under ambient atmosphere with no special condition including air or mixture exclusion.

Instrumentations

The infrared (IR) spectra were recorded by using Perkin Elmer Spectrum 100 Fourier Transform Infrared Spectrophotometer via Attenuated Total Reflection (ATR) in the spectral range of 4000 cm^{-1}-400 cm^{-1}. Whilst, ^{1}H and ^{13}C nuclear magnetic resonance (NMR) were determined by Bruker Avance III 400 spectrometer ^{1}H (400MHz) and ^{13}C (100.61MHz) by using deuterated chloroform ($CDCl_3$) acting as a solvent and tetramethylsilane (TMS) as an internal standard of δ_H (0-15 ppm) and δ_C (0-200 ppm) respectively. CH elemental analysis was carried out via Vario EL Cube Elemental Analyzer to determine the percentage weight of the elements of carbon and hydrogen presence in the synthesized compound. The UV-Vis spectroscopy spectrum was observed by using Spectrophotometer Shimadzu UV-1800 PC in 1 cm^3 quartz cuvette in dichloromethane solution with concentration of 1×10^{-5} M in the spectra range of 200–500 nm for absorbance analysis. The optimized molecular structure was obtained via density functional theory (DFT) calculation using ab initio quantum mechanical software of Gaussian 09 with correlation functional of B3LYP with basis set of 6-31G (d, p). Then, the excitation energies and correlation absorption wavelength were calculated through TD-DFT quantum mechanical calculation to obtain the energy level of HOMO-LUMO energy transition. The thermal stability was recorded via Perkin Elmer TGA Analyzer from 30 ℃ to 900 ℃ with heating rate of 10 ℃/min in the of presence nitrogen gas with flow rate of 10 mL/min. The electrochemistry was performed via AUTOLAB PGSTAT101 model potentiostat driven by NOVA 2.1 software which comprises three-electrode cell system which are working electrode (glassy carbon electrode), counter electrode (platinum wire) and reference electrode (Ag/AgCl). This experimental work-up were carried out in dichloromethane solution containing 0.1 M of tetrabutylammonium hexafluorophosphate $[NBu_4]PF_6$ as a supporting electrolyte with sample concentration of 1×10^{-3} M.

Synthetic approach

The synthesis work consists of two major parts which was the formation of 4-octyloxyacetophenone **(OCT)** as a precursor and the formation of 1-(4-octoxyphenyl)-3-[4-(trifluoromethyl)phenyl]prop-2-en-1-one **(OCT-CHAL)** as a targeted compound which were synthesized via Williamson ether synthesis and Claisen-Schmidt condensation respectively as shown in Scheme 1.

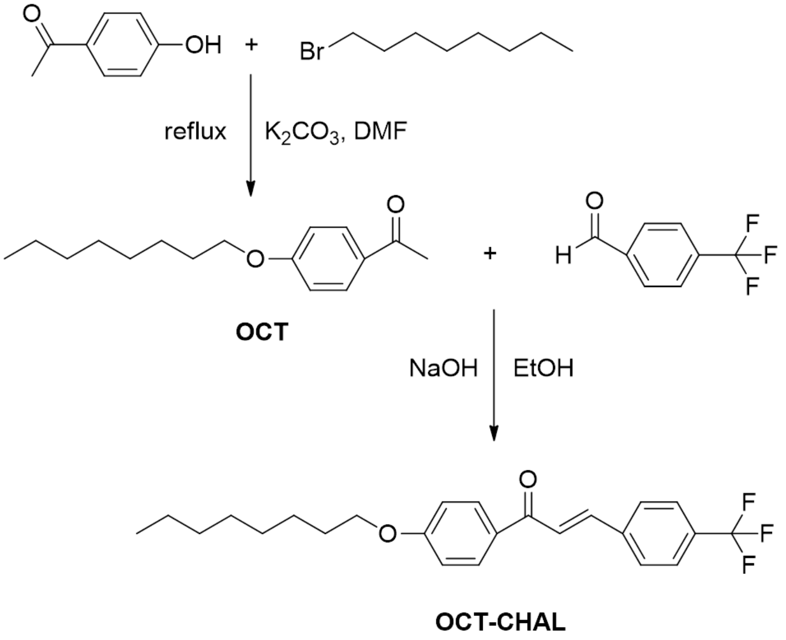

Scheme 1. Synthetic pathway for preparation of **OCT-CHAL** derivative

Synthesis of precursor: 4-octyloxyacetophenone (OCT)

Precursor of **OCT** was reported by previous literature [11], however some modifications in the experimental set-up were carried out in this study. The preparation of **OCT** was prepared by the mixture of 4-hydroxyacetophenone (1.0 g, 7.3 mmol), 1-bromooctane (1.41 g, 7.3 mmol) and potassium carbonate (3.02 g, 21.9 mmol) that were charged in 250 ml of two-necked round bottom flask. The mixture was treated with 40 ml of dimethylformamide (DMF) and was put at reflux with constant stirring for approximately 24 hours. After adjudged completion by thin layer chromatography, (TLC) (hexane: ethyl acetate; 4:1), the mixture was cooled down to room temperature and then was filtered and extracted with hexane and distilled water. The organic layer fraction obtained then was separated and washed with 1 M of aqueous NaOH (25 ml) and then with 1 M of aqueous HCl (25 ml). The organic layer obtained was dried over sodium sulphate, Na_2SO_4 and was dried *in vacuo*. (yellow viscous liquid; yield: 1.25 g, 69 %). IR (cm^{-1}): 2926.01 (*v*C-H alkanes), 2856.58 (*v*C-H alkane CH_2), 1676.14 (*v*C=O), 1598.99 (*v*C=C), 1465.90 (*v*CH_2 bend), 1357.89 (*v*CH_3 bend), 1251.80 (*v*C-O carbonyl group), 1170.79 (*v*C-O ether), 835.18 (*v*C-H aromatic OOP). ^1H NMR (400 MHz, $CDCl_3$) δ: 7.85 (pseudo-d, 2H, J = 8.8 Hz, Ar-H), 6.85 (pseudo-d, 2H, J = 9.2 Hz, Ar-H), 3.98 (t, 3H, J = 13.2 Hz, O-CH_2), 2.50 (s, 2H, H_3C-C=O), 1.75 (m, 2H, -CH_2), 1.45 (m, 2H, -CH_2), 1.25 (m, 9H, -CH_2), 0.85 (t, 3H, J = 14 Hz, -CH_3). ^{13}C NMR (100.61 MHz, $CDCl_3$) δ: 195.83, 162.11, 129.56, 129.05, 113.10, 67.24, 30.77, 28.29, 28.19, 28.07, 25.31, 24.95, 21.63, 13.08.

Synthesis of 1-(4-octoxyphenyl)-3-[4-(trifluoromethyl)phenyl]prop-2-en-1-one (OCT-CHAL)

The preparation of **OCT-CHAL** derived from the reaction of **OCT** (0.14 g, 0.8 mmol) and 4-trifluoromethylbenzaldehyde (0.2 g, 0.8 mmol) that both were charged in 250 ml of two-necked round bottom flask. The mixture was treated with 30 ml of ethanolic solution and then 20 % of NaOH was added dropwise to the mixture until the precipitate was formed under constant stirring for approximately 24 hours. When adjudged completion by thin layer chromatography, (TLC) (hexane: dichloromethane; 3:2), the mixture was poured into icy water and the cooled mixture was filtered and washed with distilled water. The precipitate collected was dried over silica gel blue before recrystallized from methanol, CH_3OH (off-white crystalline solid, 0.2 g, 55 %). IR (cm^{-1}): 2921.24 (*v*C-H alkanes), 2855.66 (*v*C-H alkane CH_2), 1664.60 (*v*C=O ketone), 1601.91 (*v*C=C alkene), 1573.94 (*v*C=C aromatic), 1470.75 (*v*CH_2 bend), 1391.65 (*v*CH_3 bend), 1328.01 (*v*C-X fluoride), 1169.85 (*v*C-O ether), 830.19 (*v*C-H aromatic OOP). ^1H NMR (400.11 MHz, $CDCl_3$) δ: 7.95 (pseudo-d, 2H, J = 8.8 Hz, Ar-H), 7.72 (d, 1H, 16 Hz, HC=CH), 7.65 (pseudo-d, 2H, 8.4 Hz, Ar-H), 7.60 (pseudo-d, 2H, 8.4 Hz, Ar-H), 7.55 (d, 1H, 16 Hz, HC=CH), 6.90 (pseudo-d, 2H, J = 9.2 Hz, Ar-H), 3.95 (t, 2H, J = 13.2 Hz, -OCH_3), 1.75 (m, 2H, -CH_2), 1.35 (m, 2H, -CH_2), 1.20 (m, 9H, -CH_2), 0.85 (t, 3H, J = 10 Hz, -CH_3). ^{13}C NMR (100.61 MHz, $CDCl_3$) δ: 187.14, 162.36, 140.76 130.17, 129.44, 127.38, 124.86, 124.82, 123.16, 113.41, 67.35, 30.78, 28.30, 28.19, 28.08, 24.97, 21.63, 13.07.

Results and Discussion

Infrared spectroscopy analysis

The spectral data of **OCT-CHAL** were recorded and analysed spectroscopically. In IR spectrum of chalcone derivative as depicted in Figure 2, it revealed all the expected bands of interest *v*(C-H alkanes), *v*(C-H alkanes, -CH_2), *v*(C=O), *v*(C=C aromatic) and *v*(C=C alkenes). The medium intensity at 2921.24 cm^{-1} and 2855.66 cm^{-1} were corresponded to vibrational of *v*(C-H alkanes). The sharp peak of IR band was observed at 1664.60 cm^{-1} and 1601.91 cm^{-1} which assigned to *v*(C=O) and *v*(C=C) with good agreement to previous researchers [12]. The medium intensity at 1573.94 cm^{-1} shows the vibrations of *v*(C=C aromatic) while strong band at 1328.01 cm^{-1} corresponded to *v*(C-X fluoride), in which the absorption of its wavenumber increase with increment of force constant from C-F bonds due to the inductive effect between C-F bond and fluorine that are attracted by fluorine electrons [13], and the vibrational of *v*(C-O) ether revealed at 1169.85 cm^{-1}.

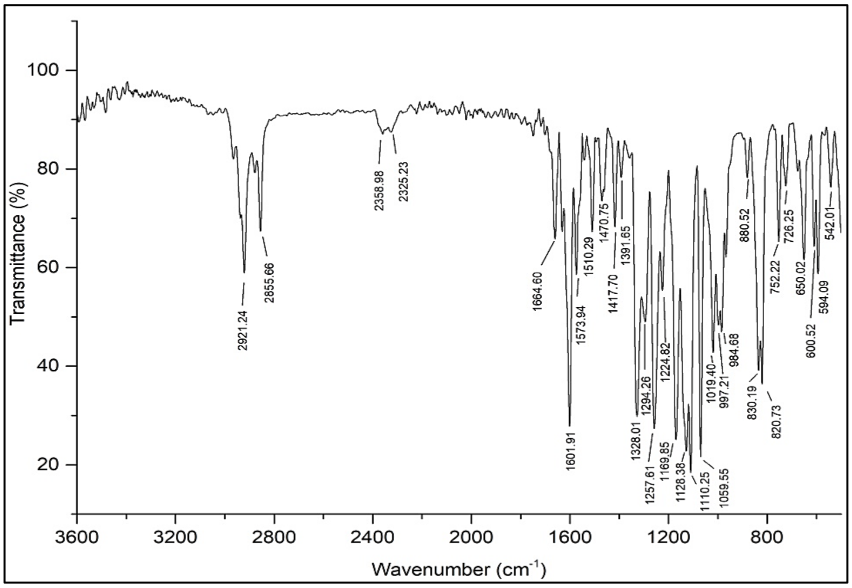

Figure 2. IR spectrum of **OCT-CHAL**

^1H and ^{13}C nuclear magnetic resonance analysis

In ^1H NMR, it revealed a pseudo-doublet resonance in the range of δ_H 7.95-6.90 ppm due to aromatic protons of para-substitution at the aromatic rings. A doublet resonance can be found at δ_H 7.72 ppm and δ_H 7.55 ppm while triplet resonance at δ_H 3.95 ppm was observed as OCH_2 due to the deshielding effect of the nearby oxygen atom which is more electronegative. Multiplet overlapping resonances lies on δ_H 1.75- 1.20 ppm while triplet resonance was recorded at shielded position δ_H

0.85 ppm. Figure 3 shows the spectrum of ^{1}H NMR for **OCT-CHAL**.

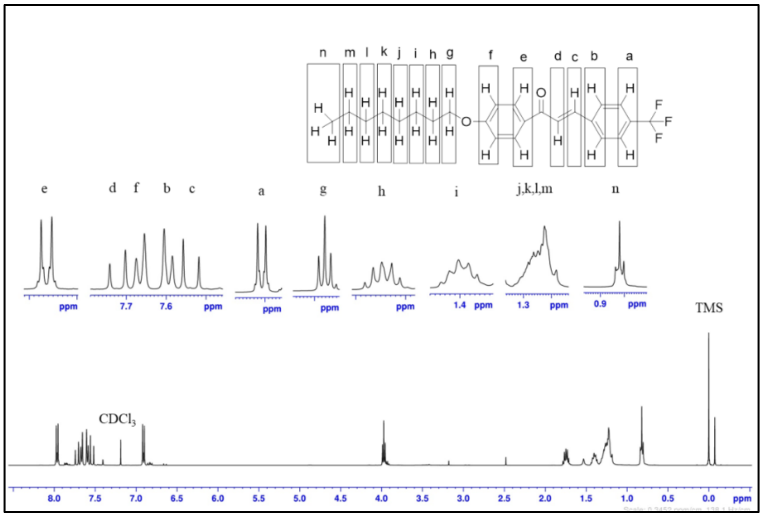

Figure 3. ^{1}H NMR spectrum of **OCT-CHAL**

The ^{13}C NMR spectrum of **OCT-CHAL** is represented in Figure 4. The C=O was identified as singlet resonance at δ_C 187.14 ppm according to deshielding effect due to the presence of nearby oxygen atom in which this trend of chemical shift position was also observed in prior reported literature [14]. Meanwhile, the aromatic carbons were recorded in the range of δ_C 162.36- 113.41 ppm. Two vinylic resonances were observed at δ_C 140.76 ppm and δ_C 123.16 ppm referring to the carbon splitting of α and β unsaturated carbons respectively due to their unsymmetrical nature within the molecular structure.

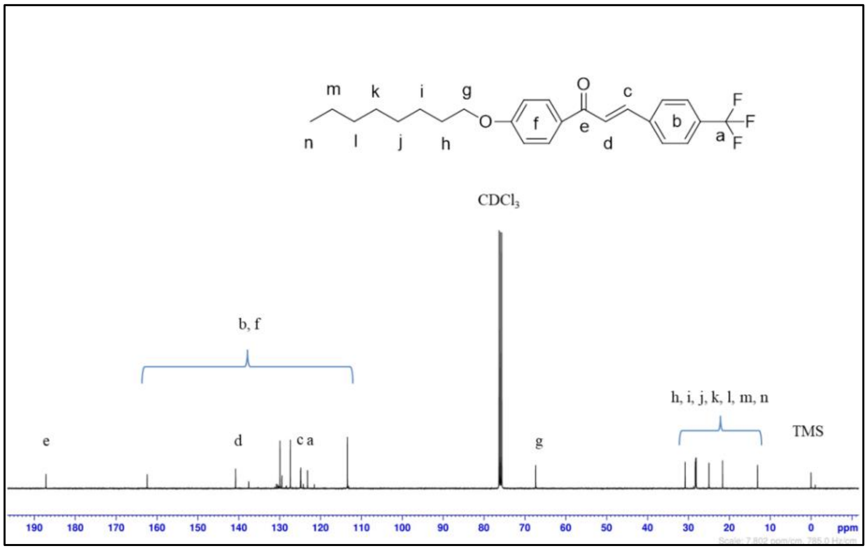

Figure 4. ^{13}C NMR spectrum of **OCT-CHAL**

Optical properties

In electronic transition of **OCT-CHAL**, it revealed π→π* transition attributed by C=O chromophore which lies in the range of 240 nm to 245 nm where the transition is shifted to longer wavelength due to the interaction of π-conjugation of carbonyl and phenyl rings. The strong absorption band between 280 nm to 330 nm can be contributed by π→π* and n→π* transitions that may correspond to C=C and C-O chromophores [8, 15]. The experimental spectrum of **OCT-CHAL** as depicted in Figure 5 (a) enables the calculation of optical band gap of this compound by referring to the formula of [E_g^{opt}= hc/ λ_{offset} (365 nm) eV]. The calculated optical band gap for **OCT-CHAL** is 3.40 eV. Comparatively, this finding has a good agreement with the values of theoretical energy band gap. The theoretical and optical band gap values are slightly different as the optical band gap are influenced by the type of solute-solvent interaction, where the solvent polarity would determine the level of ground state and excited state energy which then lead to bathochromic shift of optical spectrum. Whilst, the estimation of theoretical energy band gap was used has lowered solvatochromism in their calculation [16]. Moreover, the differences of theoretical and optical energy band gap values are also occurred due to the exciton energy binding [9], which stated that the different amount of energy band gap in the range from 0.45 eV to 1.0 eV.

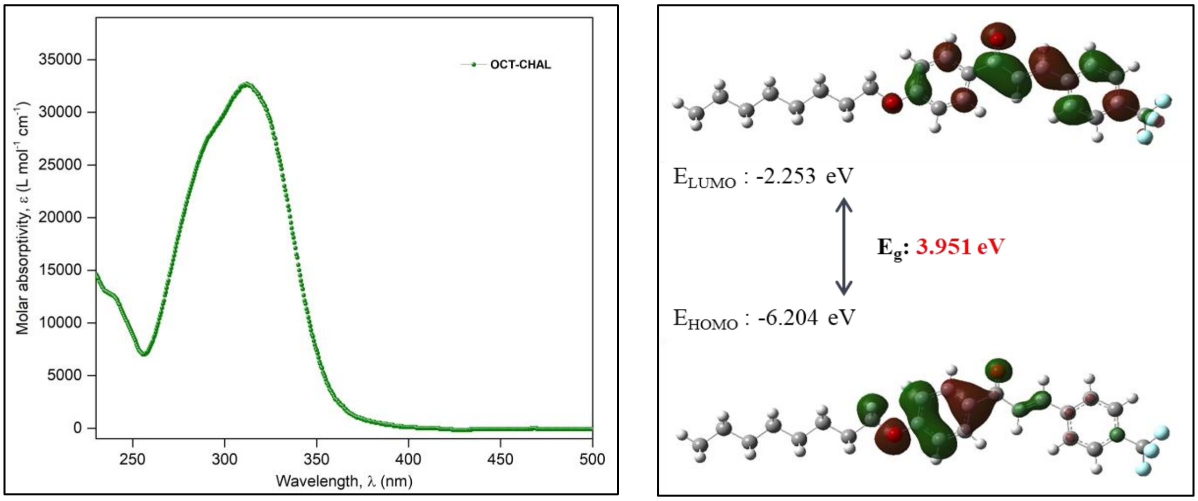

Figure 5. (a) UV-Vis spectrum of **OCT-CHAL** recorded in dichloromethane solution and (b) energy separation between HOMO-LUMO of **OCT-CHAL**

Computational calculations using time dependent density functional theory (TD-DFT) method with basis set of B3LYP-631G (d, p) was optimized from molecular structure of **OCT-CHAL** for further investigation of energy separation between the highest occupied molecular orbitals (HOMO) and lowest unoccupied molecular orbitals (LUMO). The energy separation between HOMO-LUMO energy level as depicted in Figure 5 (b). In **OCT-CHAL**, HOMO orbital density was located on electron donating alkoxy substituents while its LUMO coefficient was concentrated over enone and vinyl-substituted aryl group [17].

Molecular electrostatic potential

The molecular electrostatic potential (MEP) was performed to evaluate the molecular interaction of **OCT-CHAL**. MEP shows three-dimensional charge distributions of the molecules in which provide some information regarding to electron acceptor as well as electron donator which is displayed by colour as depicted in Figure 6. On MEP mapped surface, red area represents nucleophilic region which is rich of electron while blue area represents electrophilic region that poor of electron and green area is zero potential as it is the halfway interaction of red and blue region. The evaluation of this potential region is necessary in estimate the intermolecular and intramolecular hydrogen bonds of the molecules [17].

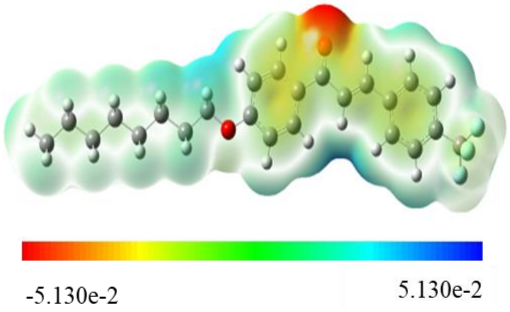

Figure 6. MEP mapped surface of **OCT-CHAL**

Global chemical reactivity descriptors

The differential global chemical reactivity descriptors (GCRD) were calculated by the evaluation of HOMO and LUMO energy level which reveal their ability as electron donor and acceptor in the compound. HOMO indicates to ionization energy (IP) while LUMO indicates to electron affinity (EA) where these findings determine the chemical properties of the molecule in term of chemical hardness (η), chemical softness (S), electronegativity (χ), chemical potential (μ) and electrophilic index (ω) as tabulated in Table 1. In addition, the calculation of HOMO-LUMO energy band gap determine the reactivity and stability of the molecule where the large optical energy band gap corresponding to less reactive and more stable and vice versa [15]. The stated parameters were used in measure the stabilities energy and reactivity of a molecule and the calculation of their quantum mechanical stabilities were calculated by equation as reported by previous literature [18, 19].

The calculation of Chemical hardness, [$\eta = (IP\text{-}EA) / 2$];
The Chemical Softness of the molecules evaluated as, [$S = 1 / 2\eta$];
The electronegativity of the molecule estimated as, [$\chi = (IP+EA) / 2$];
The chemical potential of the molecules calculated as, [$\mu = -\chi$];
The value of electrophilic index, [$\omega = \mu^2 / 2\eta$]

Table 1. Chemical properties of **OCT-CHAL** via GCRD calculation

Parameter	**[DFT-B3LYP/6–31G (d, p)]**
E_{HOMO} (eV)	-6.204
E_{LUMO} (eV)	-2.253
ΔE (eV)	3.951
Ionization potential I (eV)	6.204
Electron affinity EA (eV)	2.253
Chemical hardness η (eV)	1.976
Chemical Softness S (eV^{-1})	0.253
Electronegativity χ (eV)	4.229
Chemical potential μ (eV)	-4.229
Electrophilic index ω (eV)	4.525

Thermal studies

Thermal stability of **OCT-CHAL** was determined by thermogravimetric analyzer (TGA) where the molecule is stable up to 200 ℃ with two stages of major mass loss in the degradation process as shown in Figure 7. By observing the thermogram, the first degradation was occurred at around 201.47 ℃ (T_{onset}) and ended at 420.38 ℃ whilst second degradation was taken place at around 499.46 ℃ and ended at 570.16 ℃ with total mass loss of 97 %. Hence, the targeted alkoxylated-chalcone system of **OCT-CHAL** exhibits thermal stability at satisfactory temperature and gives good indication for the fabrication of thin film to be applied in any potential advanced materials application.

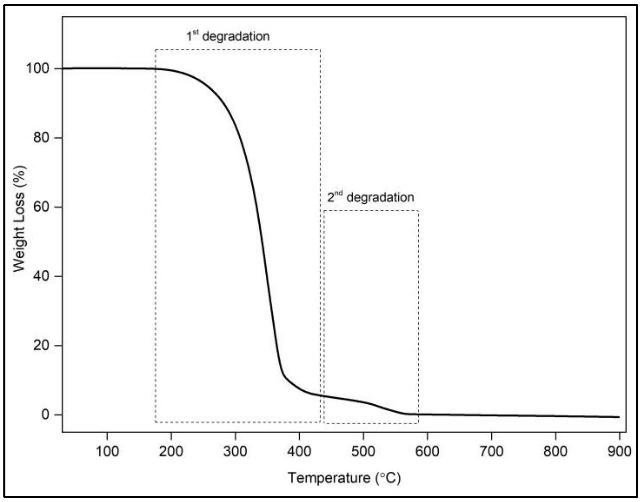

Figure 7. TGA of **OCT-CHAL**

Electrochemical properties

Cyclic Voltammetry (CV) analyzer was used in the evaluation of redox potential (oxidation and reduction) of **OCT-CHAL**. The measurement was carried out in dichloromethane solution with the presence of 0.1 M of tetrabutylammonium hexafluorophosphate, $[NBu_4]$ PF_6 acting as supporting electrolyte in the potential range of -3.0 V to 3.0 V as shown in Figure 8. From the cyclic voltammogram, the oxidation potential took place around 2.40 V at anodic peak which corresponding to oxidation of chalcone derivative due to the absorption of chalcone and/or oxidation of product occurred on the electrode surface [20]. The reduction of C=O may be corresponding to the peak revealed in the range of -1.30 V to -2.0 V with quasi-reversible reduction [21] and the process of quasi-reversibility reduction was determined by the calculation of energy separation between cathodic peak potential (E_{pa}= -1.55 V) with anodic peak potential which are (E_{pc}= -1.72 V). In addition, Ilhan and his team have confirmed this classification by evaluating the ratio of anodic peak current-to-cathodic peak current that are almost unity [22], with the values of (ΔE_p= 0.17 V).

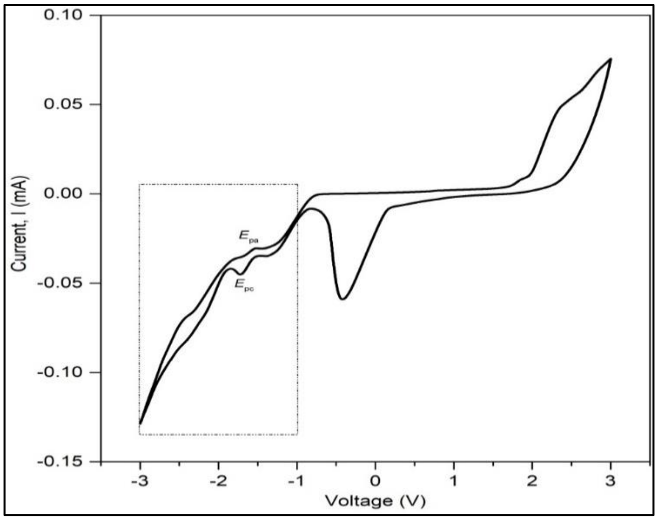

Figure 8. Cyclic voltammogram of **OCT-CHAL** in DCM/ 0.1 [NBu$_4$]PF$_6$ with scan rate of 0.03 Vs^{-1}

Conclusion

A new alkoxylated-chalcone derivative featuring donor (D)-π-Acceptor (A) system has been successfully designed and synthesized via Claisen-Schmidt condensation. The semiconductor property of **OCT-CHAL** was investigated via optoelectronic using UV-Vis spectroscopy and DFT calculation. The preliminary result reveals that this derivative exhibited an optical band gap of 3.40 eV which showed good relationship between the experimental and theoretical data. The simulated data from frontier molecular orbitals (FMO) analysis, chemical reactivity and molecular electrostatic potential (MEP) also demonstrated that this chalcone based with alkoxy substituent significantly gives good HOMO-LUMO gap which lies in the range of organic semiconducting material. Hence, from this finding, **OCT-CHAL** has proven to exhibit favourable properties for advanced material applications in the near future.

Acknowledgement

The authors would like to thank the financial support from Minister of Higher Education (MOHE) for Fundamental Research Grant (FRGS59515), FRGS/1/2018/STG07/UMT/02/6 as well as Faculty of Science and Marine Environment, Faculty of Ocean Engineering and Institute of Marine Biotechnology (IMB), Universiti Malaysia Terengganu for facilities and research aids.

References

1. Chen, F. C. (2018). Organic semiconductors. Encyclopedia of Modern Optics, Elsevier: pp. 220-231.
2. Fayed, T. A. (2006). A novel chalcone-analogue as an optical sensor based on ground and excited states intramolecular charge transfer: A combined experimental and theoretical study. *Chemical Physics*, 324 (2-3): 631-638.
3. Bangal, P. R., Lahiri, S., Kar, S. and Chakravorti, S. (1996). Vibronic interaction and photophysics of chalcone derivatives. *Journal of Luminescence*, 69(1): 49-56.
4. Kagatikar, S. and Sunil, D. (2021). Aggregation induced emission of chalcones. *Chemical Papers*, 75(12): 6147-6156.
5. Coskun, D., Gunduz, B. and Coskun, M. F. (2019). Synthesis, characterization and significant optoelectronic parameters of 1-(7-methoxy-1-benzofuran-2-yl) substituted chalcone derivatives. *Journal of Molecular Structure*, 1178: 261-267.
6. Nappi, C., Romeo, F. and Sarnelli, E. (2020). Electronic properties of one-dimensional pentacene crystals. *Nano Express*, 1 (3): 030002.

7. da Costa, R. G., Farias, F. R., Maqueira, L., Castanho, C., Carneiro, L. S., Almeida, J., Buarque, C., Aucélio, R. and Limberger, J. (2019). Synthesis, photophysical and electrochemical properties of novel D-π-D and D-π-A triphenylamino-chalcones and β-arylchalcones. *Journal of the Brazilian Chemical Society*, 30(1): 81-89.
8. Lee, S. T., Khairul, W. M., Lee, O. J., Rahamathullah, R., Daud, A. I., KuBulat, K. H., Sapari, S., Razak, F. I. A. and Krishnan, G. (2021). Electronic, reactivity and third order nonlinear optical properties of thermally-stable push-pull chalcones for optoelectronic interest: experimental and DFT assessments. *Journal of Physics and Chemistry of Solids*, 159: 110276.
9. Makhlouf, M. M., Radwan, A. S. and Ghazal, B. (2018). Experimental and DFT insights into molecular structure and optical properties of new chalcones as promising photosensitizers towards solar cell applications. *Applied Surface Science*, 452: 337-351.
10. Namal, I., Ozelcaglayan, A. C., Udum, Y. A. and Toppare, L. (2013). Synthesis and electrochemical characterization of fluorene and benzimidazole containing novel conjugated polymers: Effect of alkyl chain length on electrochemical properties. *European Polymer Journal*, 49(10): 3181-3187.
11. Nam, S. W., Kang, S. H. and Chang, J. Y. (2007). Synthesis and photopolymerization of photoreactive mesogens based on chalcone. *Macromolecular Research*, 15(1): 74-81.
12. Tay, M. G., Tiong, M. H., Chia, Y. Y., Kuan, S. H. C. and Liu, Z. Q. (2016). A way to improve luminescent efficiency of bis-chalcone derivatives. *Journal of Chemistry*, 2016: 3608137.
13. Kumar, R., Kumar, A., Deval, V., Gupta, A., Tandon, P., Patil, P. S., Desmukh, P., Chaturvedi, D. and Watve, J. G. (2017). Molecular structure, spectroscopic (FT-IR, FT Raman, UV, NMR and THz) investigation and hyperpolarizability studies of 3-(2-Chloro-6-fluorophenyl)-1-(2-thienyl) prop-2-en-1-one. *Journal of Molecular Structure*, 1129: 292-304.
14. Rahamathullah, R. and Khairul, W. M. (2017). Evaluation on the electrochemically deposited alkoxy thiourea as liquid crystalline semiconductor film. *Applied Surface Science*, 424: 45-51.
15. Veeramanikandan, S., Sherine, H. B., Dhandapani, A. and Subashchandrabose, S. (2019). Synthesis, solid state structure, Hirshfeld surface, nonlinear optics and DFT studies on novel bischalcone derivative. *Journal of Molecular Structure*, 1180: 798-811.
16. Castro, G. T., Filippa, M. A., Sancho, M. I., Gasull, E. I. and Almandoz, M. C. (2020) Solvent effect on the solubility and absorption spectra of meloxicam: experimental and theoretical calculations. *Physics and Chemistry of Liquids*, 58(3): 337-348.
17. Ustabaş, R., Süleymanoğlu, N., Özdemir, N., Kahriman, N., Bektaş, E. and Ünver, Y. (2020). New chalcone derivative: Synthesis, characterization, computational studies and antioxidant activity. *Letters in Organic Chemistry*, 17 (1): 46-53.
18. Shruthi, C., Ravindrachary, V., Guruswamy, B., Prasad, D. J., Goveas, J., Kumara, K. and Lokanath, N. K. (2021). Molecular structure, Hirshfeld surface and density functional theoretical analysis of a NLO active chalcone derivative single crystal-A quantum chemical approach. *Journal of Molecular Structure*, 1228: 129739.
19. Kumar, R., Kumar, A., Deval, V., Gupta, A., Tandon, P., Patil, P. S., Deshmukh, P., Chaturvedi, D. and Watve, J. G. (2017). Molecular structure, spectroscopic (FT-IR, FT Raman, UV, NMR and THz) investigation and hyperpolarizability studies of 3-(2-Chloro-6-fluorophenyl)-1-(2-thienyl) prop-2-en-1-one. *Journal of Molecular Structure*, 1129: 292-304.
20. Naik, K. M. and Nandibewoor, S. T. (2012). Electrochemical behavior of chalcone at a glassy carbon electrode and its analytical applications. *American Journal of Analytical Chemistry*, 3(9): 656-663.

21. Baggio, R., Brovelli, F., Moreno, Y., Pinto, M. and Soto-Delgado, J. (2016). Structural, electrochemical and theoretical study of a new chalcone derivative containing 3-thiophene rings. *Journal of Molecular Structure*, 1123: 1-7.
22. Ilhan, S., Temel, H., Yilmaz, I. and Sekerci, M. (2007). Synthesis, structural characterization and electrochemical studies of new macrocyclic Schiff base containing pyridine head and its metal complexes. *Journal of Organometallic Chemistry*, 692 (18): 3855-3865.